Journal of Materials Chemistry

Cite this: J. Mater. Chem., 2012, 22, 7945

www.rsc.org/materials

PAPER

Synthesis and applications of novel low bandgap star-burst molecules containing a triphenylamine core and dialkylated diketopyrrolopyrrole arms for organic photovoltaics

Duryodhan Sahu,[a] Chia-Hua Tsai,[a] Hung-Yu Wei,[b] Kuo-Chuan Ho,[b] Feng-Chih Chang[c] and Chih-Wei Chu*[ad]

Received 22nd December 2011, Accepted 17th February 2012
DOI: 10.1039/c2jm16760c

In this study, we used facile synthetic routes to construct two well-defined starburst donor/acceptor conjugated small molecules with broad absorption features; in **TPAKP-2** and **TPAKP-3**, triphenylamine (TPA) moieties served as electron donor core units and dialkylated diketopyrrolopyrrole (DKP) moieties with symmetrical thiophene units served as electron acceptors, in 1 : 2 and 1 : 3 ratios, respectively. Our investigation of the photophysical properties indicated that the absorption bands of **TPAKP-2**, and **TPAKP-3** extended up to 793 nm, with low optical band gaps of 1.56 and 1.65 eV respectively. Under illumination with AM 1.5 white light (100 mW cm^{-2}), we investigated the performance of bulk heterojunction (BHJ) photovoltaic devices incorporating an active layer of an electron-donor small molecule (**TPAKP-2** or **TPAKP-3**) blended with an electron acceptor: [6,6]-phenyl-C_{61}-butyric acid methyl ester ($PC_{61}BM$) or [6,6]-phenyl-C_{71}-butyric acid methyl ester ($PC_{71}BM$) at various weight ratios. The photovoltaic device containing the donor **TPAKP-3** and the acceptor $PC_{71}BM$ at a 1 : 3 weight ratio exhibited the best power conversion efficiency (1.81%), with an open circuit voltage of 0.66 V, a short circuit current density of 7.93 mA cm^{-2}, and a fill factor of 34.7%.

Introduction

Solar cells comprising organic polymers and small molecules have attracted considerable attention recently because of their attractive features such as their low cost, light weight, and large-area fabrication on flexible substrates.[1] In the last few years, studies of polymer solar cells (PSCs) based on low-bandgap polymers have dominated over small molecules because of their optimized film morphologies, higher optical densities, and higher power conversion efficiencies (PCEs).[2] Nevertheless, because of their simpler purification, controlled molecular weight distribution, and superior batch-to-batch reproducibility, small molecules are attractive for organic solar cells (OSCs) to be used as active layers.[3] With their broad absorption spectra, resulting from intramolecular charge transfer (ICT) transitions, small organic molecules featuring π-bridged donor–acceptor (D–π–A) structures are finding extensive applications in organic photovoltaics.[4] Therefore much research effort has been exerted into the development of small molecule OSCs, with a few of them exhibiting PCEs of greater than 5%.[5] To date, however, the PCEs of photovoltaic devices containing small organic molecules in the active layer remain much lower than those based on polymers. Therefore, it remains a great challenge to the research community to prepare new high performance solution-processable small organic molecules for organic photovoltaic (OPV) applications.

Among the small molecule materials tested for OSCs, the star-shaped donor π-conjugated bridge-acceptor (D–π–A) molecules stand for a novel class because of their high solution processability, high purity and chemically well-defined structures.[6–8] Furthermore, D–A–D structures in the branches of star-shaped molecules, which act as light harvesting antennae in OSC devices, could be easily tuned in their molecular structures to acquire enhanced photophysical properties.[9] Because of their high hole transporting abilities and good electron donating properties, triphenylamine (TPA) units have been used widely as efficient photovoltaic materials in OPVs.[10–12] In addition, many star-shaped molecular structures, so-called starburst molecules, have been tested for their applications in OPVs.[13,14] Besides, dialkylated diketopyrrolopyrrole (DKP)-based small-molecules and polymeric donor materials are attractive because they impart high solution-processability to the preparation of effective bulk heterojunction (BHJ) morphologies with broad absorptions in the solar spectrum.[15–17] Therefore, it is quite interesting to

[a]*Research Center for Applied Sciences, Academia Sinica, Taipei, Taiwan (ROC). E-mail: gchu@gate.sinica.edu.tw; Fax: +886-2-2782-6680; Tel: +886-2-2789-8000 ext. 70*
[b]*Institute of Polymer Science & Engineering, National Taiwan University, Taipei, 10617, Taiwan*
[c]*Department of Applied Chemistry, National Chiao-Tung University, Hsinchu, Taiwan (ROC)*
[d]*Department of Photonics, National Chiao-Tung University, Hsinchu, Taiwan (ROC)*

develop star-shaped D–π–A molecules with TPA as a core for the donor materials, and conjugated DKP arms as acceptors.

Herein, we synthesized two new starburst D–π–A molecules (**TPAKP-2** and **TPAKP-3**) featuring hole-transporting TPA donor units as the core moieties and dialkylated DKP units with symmetrical thiophene groups as the acceptor moieties in the arms. These two compounds are highly soluble in common organic solvents because of the alkyl chains present in their DKP units. Furthermore, the donor-to-acceptor ICT transitions of these star-shaped molecules (**TPAKP-2** and **TPAKP-3**) extended their absorptions up to 793 nm in the solar spectrum. In this study, the best photovoltaic performance was that of an OSC device incorporating a blend of **TPAKP-3** and $PC_{71}BM$ in a 1 : 3 weight ratio, with a highest power conversion efficiency (PCE) of 1.81%, an open circuit voltage (V_{oc}) of 0.66 V, a short circuit current density, (J_{sc}) of 7.93 mA cm^{-2}, and a fill factor (FF) of 34.7%—which are quite respectable performances for device based on a solution-processable star-shaped small molecule.

Experimental

Materials

All the chemicals were purchased from Aldrich, ACROS, Fluka, or TCI. Toluene, tetrahydrofuran (THF), and Et_2O were distilled over Na/benzophenone. $CHCl_3$ was purified by refluxing over CaH_2 followed by distillation. If not specified otherwise, the other solvents were deoxygenated by bubbling with N_2 for 1 h prior to use.

Measurements and characterization

^1H and ^{13}C NMR spectra were recorded using a Varian Unity 300 MHz spectrometer. Elemental analyses were performed using a HERAEUS CHN-OS RAPID elemental analyzer. UV–Vis absorption spectra were recorded using a HP G1103A apparatus and in dilute chlorobenzene (CB) solutions or solid films that have been spin-coated onto a glass substrate from CB solutions at a concentration of 10 mg mL^{-1}. Cyclic voltammetry (CV) was performed at room temperature using a BAS 100 electrochemical analyzer with a standard three-electrode electrochemical cell and a solution of 0.1 M tetrabutylammonium hexafluorophosphate ($TBAPF_6$) in MeCN, with a scanning rate of 100 mV s^{-1}. During the CV measurements, the solutions were purged with N_2 for 30 s. In each case, a carbon working electrode coated with a thin layer of the small molecule, a platinum wire as the counter electrode, and a silver wire as the quasi-reference electrode were used, and an Ag/AgCl (3 M NaCl) electrode served as a reference electrode for all potentials quoted herein. The redox couple of the ferrocene/ferrocenium ion (Fc/Fc^+) was used as an external standard. The corresponding energy levels of the highest occupied molecular orbital (HOMO) and the lowest unoccupied molecular orbital (LUMO) were calculated using the values of $E_{ox/onset}$ and $E_{red/onset}$ determined from solid films of the small molecules, through drop-casting films at a similar thickness from CB solutions (*ca.* 5 mg mL^{-1}). The onset potentials were determined from the intersections of two tangents drawn at the rising currents and background currents of the CV measurements. Atomic force microscopy (AFM) images of the thin films (on glass substrates) were obtained using a Digital Instruments NS 3a controller and a D3100 stage.

Fabrication of organic solar cells (OSCs)

The OSCs in this study featured an active layer of blended small molecules (**TPAKP-2** or **TPAKP-3**) blended with PCBM in solid films, which were sandwiched between a transparent indium tin oxide (ITO) anode and a metal cathode. Prior to device fabrication, the ITO-coated glass substrates (1.5 × 1.5 cm^2) were cleaned ultrasonically in detergent, deionized water, acetone, and isopropyl alcohol. After routine solvent cleaning, the substrates were treated with UV ozone for 15 min. The modified ITO surface was then obtained by spin-coating a layer of poly-(ethylene dioxythiophene): polystyrenesulfonate (PEDOT:PSS) (thickness: *ca.* 30 nm) at 130 °C for 1 h, after which the substrates were transferred into a N_2-filled glove-box. The active layer was deposited on top of the PEDOT:PSS layer through spin coating (*ca.* 2500 rpm, 60 s) of a solution of the small molecule (**TPAKP-2** or **TPAKP-3**) blended with PCBM ($PC_{61}BM$ or $PC_{71}BM$) at a ratio of 1 : 1, 1 : 2, 1 : 3, or 1 : 4 (w/w); the thickness of the active layer was typically *ca.* 80 nm. Initially, the blended solutions were prepared by dissolving both small molecules and PCBM in chlorobenzene (20 mg mL^{-1}), followed by continuous stirring for 12 h at 50 °C. In the slow-growth approach, the blends were kept in the liquid phase after spin-coating by using a solvent with a high boiling point. Finally, a Ca layer (30 nm) and an Al layer (100 nm) were thermally evaporated sequentially through a shadow mask at a pressure of less than 6 × 10^{-6} Torr. The active area of each device was 0.12 cm^2. All OSC devices were prepared and characterized under ambient conditions. The properties of the solar cells were measured inside a glove box under simulated AM 1.5G irradiation (100 mW cm^{-2}) using a Xe lamp-based solar simulator (Thermal Oriel 1000 W). The external quantum efficiency (EQE) spectra were obtained under short-circuit conditions. The light source was a 450 W Xe lamp (Oriel Instruments, model 6266) equipped with a water-based IR filter (Oriel). The light source was a 450 W Xe lamp (Oriel Instruments, Model 6123NS). The light output from the monochromator (Oriel Instruments, Model 74100) was focused on the photovoltaic cell being tested.

Fabrication of hole- and electron-only devices

The hole- and electron-only devices tested in this study contained the blend films **TPAKP-3**:$PC_{71}BM$ (in various ratios) sandwiched between the transparent ITO anode and cathode. The devices were prepared following the same procedure as the fabrication of the BHJ devices except that in the hole-only devices, Ca was replaced (with MoO_3 with work function (Φ) of 5.3 eV) and in the electron-only devices, the PEDOT:PSS layer was replaced with Cs_2CO_3 with Φ of 2.9 eV. In the hole-only devices, MoO_3 was thermally evaporated to a thickness of 20 nm and then capped with 50 nm of Al on top of the active layer. In the electron-only devices, Cs_2CO_3 was thermally evaporated with a thickness of approximately 2 nm on top of the transparent ITO. For both devices, annealing of the active layer was performed at 130 °C for 20 min. The space-charge limited current (SCLC) method was used to evaluate the hole and electron mobilities of

the small-molecule blend films of **TPAKP-3**:$PC_{71}BM$ at various weight ratios (1 : 1, 1 : 2, 1 : 3, and 1 : 4) by fabricating the hole- and electron-only devices. The electron and hole mobilities were determined precisely by fitting the plots of the dark current *versus* voltage (*J*–*V*) curves for single-carrier devices to the SCLC model. The dark current is given by:

$$J = 9\varepsilon_0\varepsilon_r \mu V^2/8L^3$$

where $\varepsilon_0\varepsilon_r$ is the permittivity of the polymer, μ is the carrier mobility, and L is the device thickness.

Synthesis

2,5-Bis(2-ethylhexyl)-3,6-di(thiophen-2-yl)pyrrolo[3,4c] pyrrole-1,4(2*H*,5*H*)-dione(2). In an oven-dried two-necked 250 mL round-bottom flask, a mixture of 3,6-dithiophen-2-yl-2,5-dihydro-pyrrolo[3,4-c]pyrrole-1,4-dione (**1**, 5.00 g, 16.90 mmol) and anhydrous K_2CO_3 (7.60 g, 54.90 mmol) were dissolved in anhydrous *N*,*N*-dimethylformamide (DMF, 120 mL) and was heated at 120 °C under N_2 for 1 h. 3-(Bromomethyl)heptane (9.80 g, 50.7 mmol) was then added dropwise, followed by a small amount of 18-crown-6. The reaction mixture was further stirred at 150 °C overnight, before being cooled to room temperature and poured into distilled water (400 mL). After stirring the resulting suspension at room temperature for 1 h, the solid was collected by vacuum filtration, washed with several portions of distilled water and methanol, and then dried under vacuum. The crude product was purified chromatographically (SiO_2; hexane–EtOAc, 4 : 1) to yield a dark red solid (6.65 g, 75%). ^{1}H NMR (300 MHz, $CDCl_3$), δ (ppm): 8.89 (dd, J = 3.9 Hz, 1.2 Hz, 2H), 7.63 (dd, J = 4.8 Hz, 0.9 Hz, 2H), 7.27 (dd, J = 6.3 Hz, 3.9 Hz, 2H), 4.04–3.96 (m, 4H), 1.87–1.83 (m, 2H), 1.38–1.24 (m, 16H), 0.87 (t, J = 7.2 Hz, 12H).

3-(5-Bromothiophen-2-yl)-2,5-bis(2-ethylhexyl)-6-(thiophen-2-yl)pyrrolo[3,4-c]pyrrole-1,4(2*H*,5*H*)-dione (3). *N*-Bromosuccinimide (NBS, 1.70 g, 9.52 mmol) was added in portions to a solution of **2** (5 g, 9.52 mmol) in $CHCl_3$ (100 mL) in a two-necked flask at 5 °C. The mixture was warmed to room temperature and stirred overnight. CH_2Cl_2 was added and then the solution was washed with brine. The organic phase was dried ($MgSO_4$) and the solvent was evaporated under reduced pressure. The crude product was purified chromatographically (SiO_2;hexane–EtOAc, 1 : 1) to yield a red solid (3.30 g, 58%). ^{1}H NMR (300 MHz, $CDCl_3$), δ (ppm): ^{1}H NMR (300 MHz, $CDCl_3$), δ (ppm): 8.90 (dd, J = 3.9 Hz, 1.2 Hz, 1H), 8.63 (d, 4.2 Hz, 1H) 7.64 (dd, J = 5.1 Hz, 1.2 Hz, 1H), 7.29–7.22 (m, 2H), 4.03–3.92 (m, 4H), 1.84 (m, 2H), 1.38–1.23 (m, 16H), 0.91–0.85 (m, 12H).

4,4′-Dibromotriphenylamine (4a). NBS (15.2 g, 81.5 mmol) was added in portions to a solution of TPA (10.0 g, 40.8 mmol) in DMF (120 mL) in a two-necked flask at 0 °C. The mixture was warmed to room temperature, stirred for an additional 12 h, and then poured into excess water and extracted with CH_2Cl_2. The combined extracts were washed with brine and dried ($MgSO_4$) and then the solvent was evaporated under reduced pressure. The residue was purified chromatographically (SiO_2; hexane–CH_2Cl_2, 5 : 1) to yield as colorless oil, which solidified when stored below room temperature (11.2 g, 68%). ^{1}H NMR (300 MHz, $CDCl_3$), δ (ppm): 7.43 (d, J = 8.7 Hz, 4H), 7.31 (t, J = 7.8 Hz, 2H), 7.11–7.01 (m, 3H), 6.91 (d, J = 8.7 Hz, 4H).

4,4′,4″-Tribromotriphenylamine (4b). This compound was prepared by the same procedure as that described for compound **4a** with 1 and 3.3 molar equivalents of TPA and NBS, respectively, to yield a white solid (yield = 90%). ^{1}H NMR (300 MHz, $CDCl_3$), δ (ppm): 7.36 (d, J = 8.3 Hz, 6H), 6.92 (d, J = 8.3 Hz, 6H).

***N*-Phenyl-4-(4,4,5,5-tetramethyl-1,3,2-dioxaborolan-2-yl)-*N*-[4-(4,4,5,5-tetramethyl-1,3,2-dioxaborolan-2-yl)phenyl] aniline (5a).** *n*-BuLi (2.5 M in hexane, 10.9 mL, 27.3 mmol) was added dropwise (using a syringe) to a solution of **4a** (5.00 g, 12.4 mmol) in anhydrous THF (80 mL) at −78 °C under N_2 and then the mixture was stirred at −78 °C for 2 h. 2-Isopropoxy-4,4,5,5-tetramethyl-1,3,2-dioxaborolane (6.32 mL, 31.0 mmol) was added in one portion to the mixture, which was then warmed to room temperature and stirred overnight. The solvent was evaporated under vacuum; the crude product was dissolved in CH_2Cl_2 (50 mL) and washed with water (3 × 50 mL). The organic phase was dried ($MgSO_4$) and the solvent was evaporated under vacuum. The residue was purified chromatographically (SiO_2, hexane–EtOAc, 20 : 1) to afford a white solid (3.63 g, 59%). ^{1}H NMR (300 MHz, DMSO-d_6), δ (ppm): 7.56 (d, J = 8.7 Hz, 4H), 7.34 (t, J = 7.8 Hz, 2H), 7.12 (t, J = 7.5 Hz, 1H), 7.04 (d, J = 7.8 Hz, 2H), 6.95 (d, J = 8.4 Hz, 4H), 1.26 (s, 24H).

Tris[4-(4,4,5,5-tetramethyl-1,3,2-dioxaborolan-2-yl) phenyl-amine (5b). This compound was prepared in the same procedure as that described for **5a** using 1 : 3.3 : 3.5 molar equivalents of **4b**, *n*-BuLi and 2-isopropoxy-4,4,5,5-tetramethyl-1,3,2-dioxaborolane, respectively, as a white solid (yield = 62%). ^{1}H NMR (300 MHz, $CDCl_3$), δ (ppm): 7.66 (d, J = 8.7 Hz, 6H), 7.07 (d, J = 8.4 Hz, 6H), 1.34 (s, 36H).

6,6′-(5,5′-(4,4′-(Phenylazanediyl)bis(4,1-phenylene))bis(thiophene-5,2-diyl))bis(5-(2-ethylhexyl)-2-(octan-3-yl)-3-(thiophen-2-yl)pyrrolo[3,4-c]pyrrole-1,4(2*H*,5*H*)-dione) (TPAKP-2). A mixture of compound **5a** (0.5 g, 1.00 mmol), compound **3** (1.39 g, 2.3 mmol), and 2 M K_2CO_3 (360 mg, 2.6 mmol) were dissolved in 30 mL of toluene and ethanol (3 : 1)followed by $Pd(PPh_3)_4$ (45 mg, 0.04 mmol) and degassed for 10 min. The resulting mixture was then stirred under reflux for 36 h. The solvent was evaporated under vacuum and the residue was partitioned between CH_2Cl_2 and water; the organic phase was washed with brine and dried ($MgSO_4$) and then the solvent was evaporated under vacuum. The residue was purified chromatographically (SiO_2; CH_2Cl_2) and the product was washed with MeOH and hexane to yield a black solid (0.71 g, 55%). ^{1}H NMR (300 MHz, $CDCl_3$), δ (ppm): 9.00 (d, J = 4.2 Hz, 2H), 8.87 (d, J = 3.9 Hz, 2H), 7.62–7.56 (m, 5H), 7.40 (d, J = 4.2 Hz, 2H), 7.36–7.31 (m, 2H), 7.28–7.25 (m, 3H), 7.20–7.13 (m, 7H), 4.04 (m, 8H), 1.92 (m, 6H), 1.41–1.23 (m, 30H), 0.93–0.83 (m, 24H). ^{13}C NMR (75 MHz, $CDCl_3$): δ 162.1, 161.8, 149.9, 148.0, 146.7, 140.7, 139.8, 137.5, 135.2, 130.5, 130.1, 129.9, 128.6, 128.2, 127.8, 127.3, 125.7, 124.7, 124.1, 124.0, 108.4, 108.0, 46.2, 39.4, 39.3, 30.5, 30.4, 29.5, 28.7, 28.5, 25.0, 23.9, 23.7, 23.3, 14.3, 14.2, 10.8, 10.7.

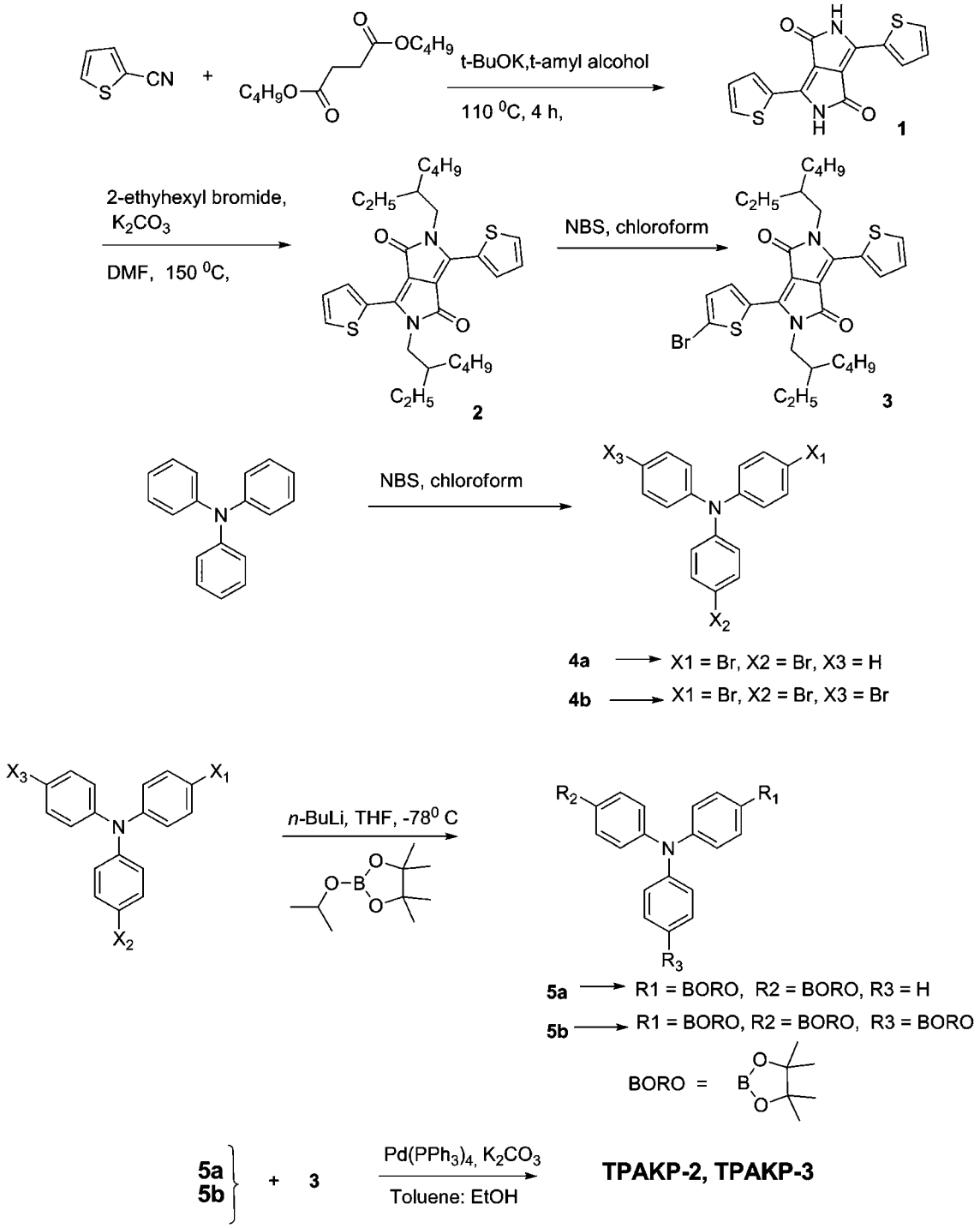

Scheme 1 Synthesis of **TPAKP-2** and **TPAKP-3**.

MS (FAB): *m/z* [M$^+$] 1290; calcd *m/z* 1289.60. Anal. Calcd for $C_{78}H_{91}N_5O_4S_4$: C, 72.58; H, 7.11; N, 5.43. Found: C, 71.89; H, 6.90; N, 5.12.

6,6′,6″-{5,5′,5″-[4,4′,4″-Nitrilotris(benzene-1,4-diyl)]tris (thiophene-5,2-diyl)}tris[2,5-bis(2-ethylhexyl)-3-(thiophen-2-yl)pyrrolo [3,4-c]pyrrole-1,4(2*H*,5*H*)-dione] (TPAKP-3). This compound was prepared, using 1 : 3.5 molar equivalents of compound **5b** and **3** and in the same procedure as that was described for **TPAKP-2**, to yield a black solid (yield = 62%). ^{1}H NMR (300 MHz, $CDCl_3$), δ (ppm): 9.00 (d, J = 4.2 Hz, 3H), 8.87 (dd, J = 3.9 Hz, 1.2 Hz, 3H), 7.62 (d, J = 1.2 Hz, 8H), 7.61 (d, J = 1.5 Hz, 3H), 7.28–7.25 (m, 4H), 7.20 (m, 6H), 4.03 (m, 12H), 1.94–1.85 (m, 6H), 1.41–1.26 (m, 48H), 0.90–0.83 (m, 36H). ^{13}C NMR (75 MHz, $CDCl_3$): δ 162.0, 161.9, 149.5, 147.3, 140.5, 140.0, 137.4, 135.3, 130.6, 130.2, 128.7, 128.6, 128.5, 127.5, 124.9,

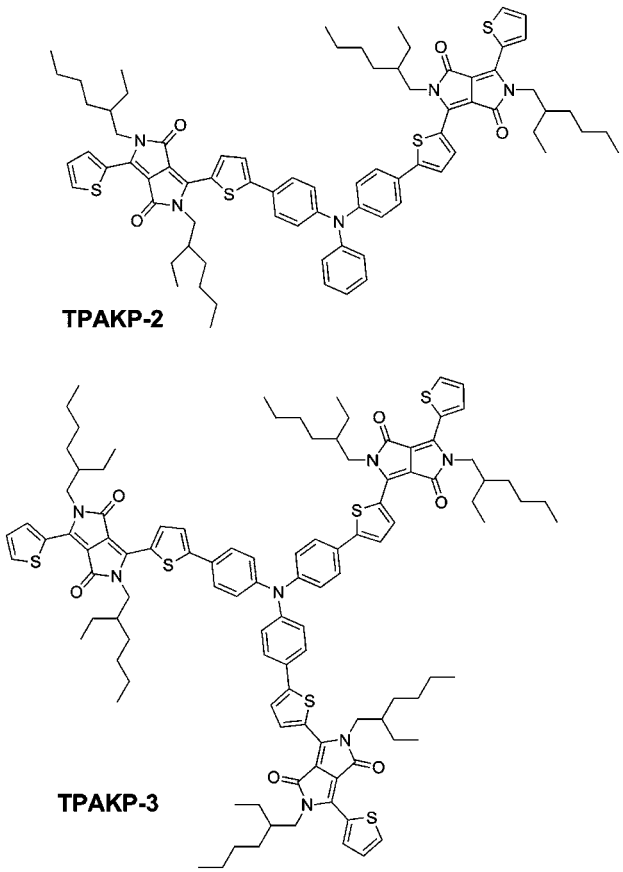

Fig. 1 Molecular structures of **TPAKP-2** and **TPAKP-3**.

124.2, 108.4, 108.1, 46.1, 39.4, 39.3, 30.5, 30.4, 28.7, 28.5, 23.9, 23.8, 23.3, 14.3, 14.2, 10.8, 10.7. MS (FAB): *m/z* [M^+] 1812; calcd *m/z* 1811.83. Anal. Calcd for $C_{108}H_{129}N_7O_6S_6$: C, 71.52; H, 7.17; N, 5.41. Found: C, 70.80; H, 7.01; N, 5.56.

Results and discussion

Synthesis and structural characterization

Scheme 1 outlines the synthetic approach towards **TPAKP-2** and **TPAKP-3**; Fig. 1 depicts the structures of the final products. Compound **1** was obtained through a known procedure[18] and then reacted with 3-(bromomethyl)heptane and K_2CO_3 in DMF to provide compound **2** in 75% yield. Compounds **3**, **4a**, and **4b** were synthesized through simple brominations with NBS. The di- and tri-boronic esters of TPA (**5a** and **5b**, respectively) were prepared from the corresponding bromides after successive treatments with *n*-BuLi and 2-isopropoxy-4,4,5,5-tetramethyl-1,3,2-dioxaborolane. The final products **TPAKP-2** and **TPAKP-3** were produced through Pd(0)-catalyzed Suzuki couplings of compound **3** with **5a** and **5b**, respectively. Both **TPAKP-2** and **TPAKP-3** were soluble in common organic solvents, including CH_2Cl_2, $CHCl_3$, THF, CB, and dichlorobenzene.

Optical properties

We used UV–Vis spectroscopy to investigate the optical properties of the D–π–A molecules **TPAKP-2** and **TPAKP-3** in CB solutions (Fig. 2a) as well as in the solid films (Fig. 2b); Table 1 lists the pertinent data. In solution, both compounds exhibited two absorption bands: one at 340 nm for **TPAKP-2** and 349 nm for **TPAKP-3** for the π–π* transitions of their conjugated backbones, and the other at 598 nm for **TPAKP-2** and 601 nm for **TPAKP-3** representing the ICT transitions between their TPA cores and the branched DKP acceptors.[19] In the spectra of the solid films, the absorption maxima of both the low- and high-energy bands of **TPAKP-2** and **TPAKP-3** were bathochromically shifted relative to those in solution. These bathochromic shifts were attributed to the intermolecular interactions in the solid state. The UV–Vis absorption spectra of the solutions revealed that the net molar extinction coefficient of **TPAKP-3** was greater than that of **TPAKP-2** (Fig. 2a, Table 1). In addition, the absorption intensity of **TPAKP-3** (Fig. 2b) in solid film (thickness: *ca.* 100 nm) was greater then that of **TPAKP-2** (thickness: *ca.* 100 nm), confirming that **TPAKP-3** had a higher optical density and could absorb a greater number of photons from the solar spectrum than could **TPAKP-2**; this behavior was also reflected as higher photocurrent densities of the photovoltaic devices incorporating **TPAKP-3** as the active layer.[20] In addition, the absorption onset of **TPAKP-3** ($\lambda_{onset,film}$ = 793 nm) was bathochromically shifted by 44 nm relative to that of **TPAKP-2**

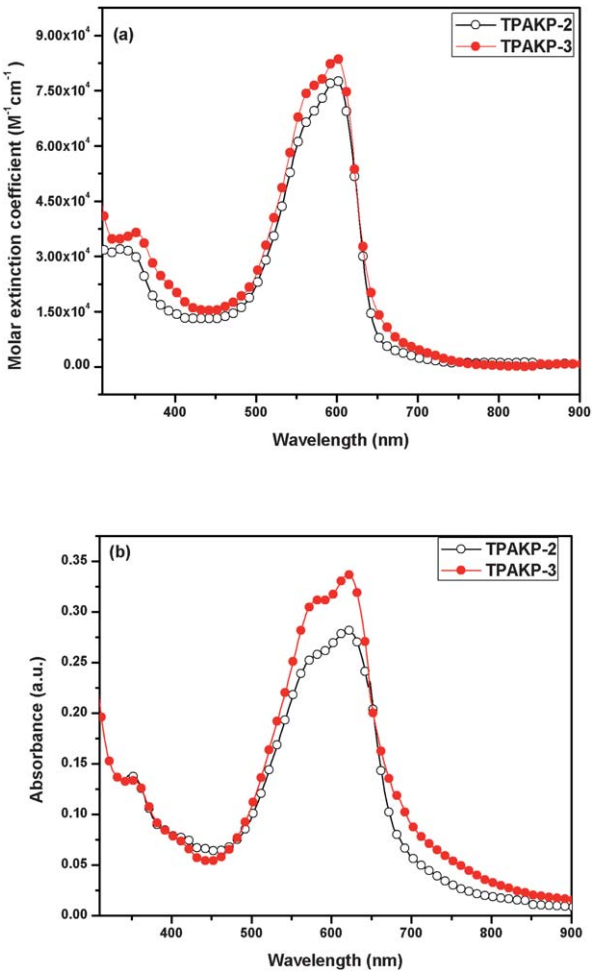

Fig. 2 UV–Vis absorption spectra of **TPAKP-2**, and **TPAKP-3** in (a) dilute chlorobenzene solutions and (b) solid films.

Table 1 Optical properties of **TPAKP-2** and **TPAKP-3**

Small molecule	$\lambda_{abs,sol}$/nm[a], ($\varepsilon \times 10^4$/M^{-1} cm^{-1})	$\lambda_{abs,film}$/nm[b]	$\lambda_{onset,film}$/nm	$E_{g,film}^{opt}$/eV[c]
TPAKP-2	340, (3.11); 598 (7.73)	348, 620	749	1.65
TPAKP-3	349, (3.61); 601 (8.39)	354, 622	793	1.56

[a] In dilute chlorobenzene solution. [b] Spin-coated from chlorobenzene solutions. [c] Optical bandgaps were determined using the equation $E_{g,film}^{opt} = 1240/\lambda_{onset,film}$.

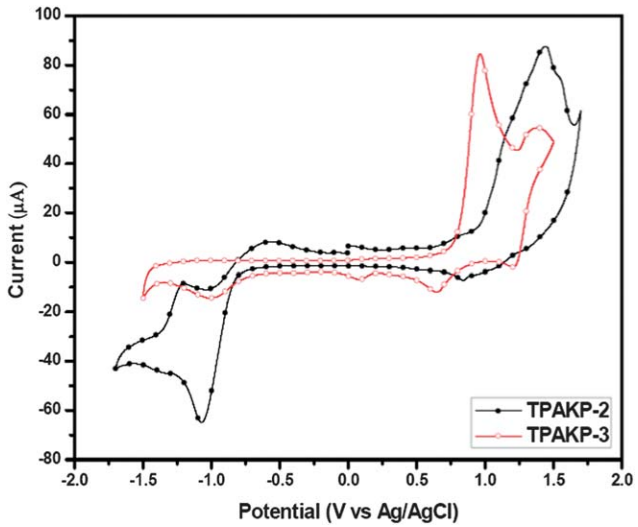

Fig. 3 Cyclic voltammograms of **TPAKP-2** and **TPAKP-3** films (drop cast) on Pt electrodes measured under 0.1 M ((TBA)PF_6) MeCN at a scan rate of 100 mV s^{-1}.

($\lambda_{onset,film}$ = 749 nm), but there were no significant changes in their absorption maxima (λ_{abs}). Furthermore, the broadening of the value of λ_{onset}, due to the ICT from the donor core to the acceptor arms, decreased the optical band gap from 1.65 eV for **TPAKP-2** to 1.56 eV for **TPAKP-3** (Table 1).

Electrochemical properties

To study the electronic structures of the D–π–A star-shaped molecules **TPAKP-2** and **TPAKP-3**, we determined the HOMO and LUMO energy levels through CV measurements of their solid films with Ag/AgCl as a reference electrode, calibrated by ferrocene ($E_{1/2(ferrocene)}$ = 0.45 V *vs.* Ag/AgCl).

We estimated the HOMO and LUMO energy levels from the oxidation and reduction potentials relative to the reference energy level of ferrocene (4.8 eV below the vacuum level) according to the equation:[21]

$$E_{HOMO/LUMO} = [-(E_{onset} - 0.45) - 4.8]\ eV$$

As summarized the results in Fig. 3 and Table 2. The HOMO/LUMO energy levels of **TPAKP-2** and **TPAKP-3** were −5.20/−3.53 eV and −5.15/−3.60 eV, respectively. As expected, the introduction of electron withdrawing groups on the branches of the star-shaped molecules decreased the bandgaps by lowering the LUMO energy levels; the band gaps for **TPAKP-2** and **TPAKP-3** were 1.67 and 1.55 eV, respectively. The electrochemical bandgaps found were in good agreement with the obtained optical bandgaps and also in the desirable range for use in organic photovoltaic applications.[22]

Photovoltaic properties

We explored the potential applications of the D–π–A molecules **TPAKP-2** and **TPAKP-3** in OSCs by fabricating BHJ photovoltaic devices with the configuration ITO/PEDOT:PSS (30 nm)/**TPAKP-2** or **TPAKP-3**:$PC_{61}BM$ blend (*ca.* 80 nm)/Ca (30 nm)/Al (100 nm).

The solutions for the active layer were prepared by blending **TPAKP-2** or **TPAKP-3** with $PC_{61}BM$ at various weight ratios (1 : 1, 1 : 2, 1 : 3, 1 : 4) initially and the active layer compositions were later modified using various weight ratios of the better-performing molecule (**TPAKP-3**) blended with $PC_{71}BM$ (owing to its broader absorption and higher absorption coefficient, relative to $PC_{61}BM$). Table 3 lists the photovoltaic properties (V_{oc}, J_{sc}, FF, PCE) of the PSC devices based on **TPAKP-2** and **TPAKP-3** with $PC_{61}BM$ at the various weight ratios. We found that blending of the D–π–A molecule, possessing three arms (**TPAKP-3**) with $PC_{61}BM$ (1 : 3, w/w) provided a greater PCE (1.22%)—with values of V_{oc}, J_{sc}, and FF of 0.62 V, 5.39 mA cm^{-2}, and 36.5%, respectively—than that of the device incorporating **TPAKP-2** blended with $PC_{61}BM$ (1 : 2, w/w; PCE = 0.97%; V_{oc} = 0.58 V; J_{sc} = 4.88 mA cm^{-2}; FF = 34.3%). We attribute these enhanced properties to the star-shaped molecule **TPAKP-3** featuring a greater number of arms, which acted as better light harvesting antennae and helped to adsorb a greater number of photons, thereby providing a higher value of J_{sc} (5.39 mA cm^{-2}) than that (4.88 mA cm^{-2}) of the device

Table 2 Electrochemical properties of **TPAKP-2** and **TPAKP-3**

Small molecules	$E_{ox,onset}$/V[a]	$E_{red,onset}$/V[a]	E_{HOMO}/eV[b]	E_{LUMO}/eV[b]	E_g^{CV}/eV
TPAKP-2	0.85	−0.82	−5.20	−3.53	1.67
TPAKP-3	0.80	−0.75	−5.15	−3.60	1.55

[a] Onset oxidation and reduction potentials measured by cyclic voltammetry in solid films. [b] $E_{HOMO}/E_{LUMO} = [-(E_{onset} - 0.45) - 4.8]$ eV, where 0.45 V is the value for ferrocene *vs.* Ag/Ag^+ and 4.8 eV is the energy level of ferrocene below the vacuum.

Table 3 Photovoltaic properties of BHJ solar cell devices having the configuration of ITO/PEDOT:PSS/small molecule:$PC_{61}BM$/Ca/Al[a]

Small molecule	Small molecule/$PC_{61}BM$	V_{oc}/V	J_{sc}/mA cm^{-2}	FF (%)	PCE (%)
TPAKP-2	1 : 1	0.58	4.23	34.2	0.84
	1 : 2	0.58	4.88	34.3	0.97
	1 : 3	0.55	4.65	34.4	0.88
	1 : 4	0.51	4.04	34.5	0.71
TPAKP-3	1 : 1	0.63	3.26	32.1	0.66
	1 : 2	0.64	4.41	33.7	0.95
	1 : 3	0.62	5.39	36.5	1.22
	1 : 4	0.69	4.72	35.3	1.15

[a] Measured under AM 1.5 irradiation, 100 mW cm^{-2}.

incorporating **TPAKP-2**. In addition, the donor/acceptor blending ratio also played a key role in determining the photovoltaic properties.[23] As revealed in Table 3, **TPAKP-2** (two acceptor branches) and **TPAKP-3** (three acceptor branches) required 1 : 2 (w/w; 1 : 3 molar ratio) and 1 : 3 (w/w; 1 : 6 molar ratio) of small molecule-to-$PC_{61}BM$ blend ratios, respectively, to provide their optimal PCEs (0.97 and 1.22%, respectively). The higher molar ratio (1 : 6) for the three-dimensional spatial structure of the donor (**TPAKP-3**) and $PC_{61}BM$ provided intimate intermixing and resulted in very efficient exciton dissociation and, thereby, charge carrier generation throughout the whole volume of the blend. In theory, the value of V_{oc} is dependent on the difference between the HOMO energy level of the donor and the LUMO energy level of the acceptor. We found, however, that the values of V_{oc} for the devices incorporating **TPAKP-2** and **TPAKP-3** deviated from theory, presumably because of carrier recombination or resistance related to the thickness of the active layer.[24]

The performance of the PSC devices containing **TPAKP-3** was optimized by fabricating BHJ OSC devices featuring **TPAKP-3** (donor) and $PC_{71}BM$ (acceptor) in various weight ratios (1 : 1, 1 : 2, 1 : 3, 1 : 4). The *J*–*V* curves and the external quantum efficiency (EQE) curves of the devices based on **TPAKP-3**:$PC_{71}BM$ in these four different blended ratios are shown in Fig. 4 and 5, respectively, and the data are illustrated in Table 4.

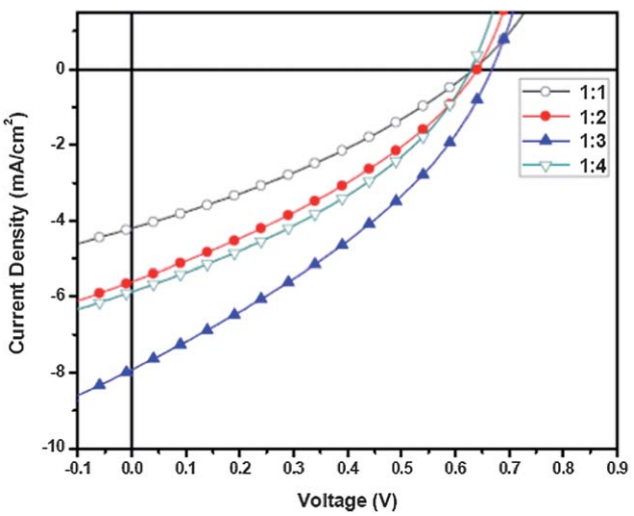

Fig. 4 Current–voltage (*J*–*V*) curves of BHJ solar cells incorporating **TPAKP-3**/$PC_{71}BM$ blends at various weight ratios under AM 1.5G illumination (100 mW cm^{-2}).

The PSC device based on **TPAKP-3**:$PC_{71}BM$ at a 1 : 3 weight ratio provided the best PCE value (1.81%) with values of V_{oc}, J_{sc}, and FF of 0.66 V, 7.92 mA cm^{-2}, and 34.7%, respectively. The devices based on blends of **TPAKP-3**:$PC_{71}BM$ at 1 : 1, 1 : 2 and 1 : 4 weight ratios displayed relatively poor photocurrent responses and EQEs (see Fig. 5), presumably because of suppressed charge separation and transportation within the active layer. Furthermore, the poor and unbalanced (by two orders of magnitude) hole and electron mobilities in the device containing **TPAKP-3**/$PC_{71}BM$ at a 1 : 4 weight ratio built up the space charge and limited the net photocurrent, thereby contributing (see Table 4) to the net decrease in its PCE.[25–27]

The device based on **TPAKP-3** blended with $PC_{71}BM$ at a 1 : 3 weight ratio exhibited the highest PCE (1.81%), which was attributed to its broader absorption spectrum (λ_{onset} = 793 nm), deeper HOMO level (E_{HOMO} = −5.15 eV), broader and higher EQE (*ca.* 41% at *ca.* 598 nm) and relatively balanced hole (μ_h = 5.21 × 10^{-7} cm^2 V^{-1} s) and electron (μ_e = 5.28 × 10^{-6} cm^2 V^{-1} s) mobilities, even though these hole and electron mobilities were low. To investigate the mixing morphologies in the films, which affect the interpenetrated networks of the donor and acceptor units, we recorded AFM images of the **TPAKP-3**:$PC_{71}BM$ blends at different weight ratios (Fig. 6). The average root-mean-square roughnesses (R_{rms}) of the films of the **TPAKP-3**/$PC_{71}BM$ blends at weight ratios of 1 : 1, 1 : 2, 1 : 3, and 1 : 4 were 0.77, 0.57, 0.32, and 0.28 nm, respectively. These values indicate that the films possessed finely mixed morphologies, regardless of the

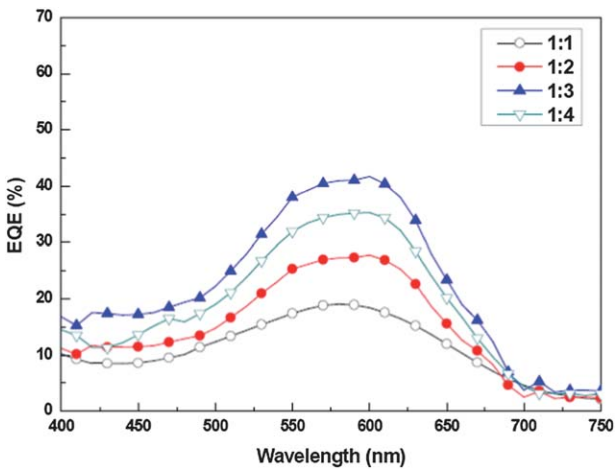

Fig. 5 EQE curves of BHJ solar cells incorporating **TPAKP-3**:$PC_{71}BM$ blends at various weight ratios.

Table 4 Photovoltaic properties of bulk heterojunction solar cell devices with a configuration of ITO/PEDOT:PSS/**TPAKP-3**:$PC_{71}BM$/Ca/Al[a]

TPAKP3:$PC_{71}BM$	μ_h/cm^2 V^{-1} s	μ_e/cm^2 V^{-1} s	V_{oc}/V	J_{sc}/mA cm^{-2}	FF (%)	PCE (%)
1 : 1	6.49×10^{-7}	8.26×10^{-6}	0.63	4.20	32.1	0.85
1 : 2	4.07×10^{-7}	3.93×10^{-6}	0.64	5.60	33.5	1.20
1 : 3	5.21×10^{-7}	5.28×10^{-6}	0.66	7.92	34.7	1.81
1 : 4	4.15×10^{-7}	3.02×10^{-5}	0.62	5.87	36.5	1.33

[a] Measured under AM 1.5 irradiation (100 mW cm^{-2}).

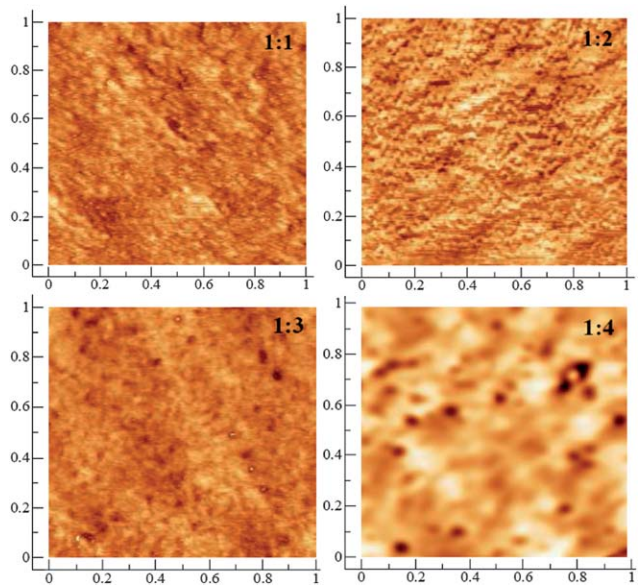

Fig. 6 AFM images of **TPAKP-3**: $PC_{71}BM$ blends at various weight ratios.

content of $PC_{71}BM$. Furthermore, we tested the effects of various annealing temperatures (from 50 to 200 °C) on the molecular order in the active layer, but found no improvements in either the values of J_{sc} or the PCE, which is consistent with the poor crystallinity and phase separation in these blends.

Nonetheless, the smoother surface of the device containing the **TPAKP-3**/$PC_{71}BM$ blend at a 1 : 3 weight ratio provided a higher diffusion escape probability for mobile charge carriers and higher short circuit currents.[24a,b] In general, it is more difficult to obtain high-quality films in small-molecule BHJ solar cells, as evidenced by the low and non-symmetric hole and electron mobilities and the poor AFM morphologies obtained upon varying the donor/acceptor weight ratios (see Table 4 and Fig. 6). It might be possible to improve the morphology of the active layer further by using solvent mixtures or high-boiling-point-solvent additives, which may further assist the formation of the interpenetrating network by enhancing the crystalline phase of the small-molecule active layer without disrupting the fullerene acceptor during drying.[28–30]

Conclusion

We have designed and synthesized two novel star-burst D–π–A structured molecules containing TPA units as cores and DKP moieties with symmetrical thiophene units as arms for application in OSCs. The absorptions in the visible region of the tri-burst molecule **TPAKP-3** were broader (covering a wavelength range from 450 to 793 nm) and stronger than those of the di-burst molecule **TPAKP-2**. Furthermore the number of accepting arms played a key role in determining their optical and photovoltaic properties. The photovoltaic device containing a blend of **TPAKP-3** and $PC_{71}BM$ in a 1 : 3 weight ratio provided to the highest PCE (1.81%) with other optimal photovoltaic performances in terms of values of V_{oc}, J_{sc}, and FF of 0.66 V, 7.93 mA cm^{-2}, and 34.7%, respectively.

Acknowledgements

We thank the National Science Council, Taiwan (NSC 100-2120-M-009-004), and the Academia Sinica Research Project on Nano Science and Technology for financial support.

References

1 (*a*) K. Walzer, B. Maennig, M. Pfeiffer and K. Leo, *Chem. Rev.*, 2007, **107**, 1233; (*b*) S. Günes, H. Neugebauer and N. S. Sariciftci, *Chem. Rev.*, 2007, **107**, 1324; (*c*) Y.-J. Cheng, S.-H. Yang and C.-S. Hsu, *Chem. Rev.*, 2009, **109**, 5868; (*d*) B. Walker, C. Kim and T.-Q. Nguyen, *Chem. Mater.*, 2011, **23**, 470.

2 (*a*) H. X. Zhou, L. Q. Yang, A. C. Stuart, S. C. Price, S. B. Liu and W. You, *Angew. Chem., Int. Ed.*, 2011, **50**, 2995; (*b*) T.-Y. Chu, J. P. Lu, S. Beaupre, Y. G. Zhang, J.-R. Pouliot, S. Wakim, J. Y. Zhou, M. Leclerc, Z. Li, J. F. Ding and Y. Tao, *J. Am. Chem. Soc.*, 2011, **133**, 4250; (*c*) S. C. Price, A. C. Stuart, L. Q. Yang, H. X. Zhou and W. J. You, *J. Am. Chem. Soc.*, 2011, **133**, 4625; (*d*) J.-H. Park, D. S. Chung, D. H. Lee, H. Kong, I. H. Jung, M.-J. Park, N. S. Cho, C. E. Park and H.-K. Shim, *Chem. Commun.*, 2010, **46**, 1863; (*e*) L. J. Huo, S. Q. Zhang, X. Guo, F. Xu, Y. F. Li and J. H. Hou, *Angew. Chem., Int. Ed.*, 2011, **50**, 9697.

3 (*a*) B. Walker, A. B. Tamayo, X. D. Dang, P. Zalar, J. H. Seo, A. Garcia, M. Tantiwiwat and T. Q. Nguyen, *Adv. Funct. Mater.*, 2009, **19**, 3063; (*b*) J. A. Mikroyannidis, S. S. Sharma, Y. K. Vijay and G. D. Sharma, *ACS Appl. Mater. Interfaces*, 2010, **2**, 270; (*c*) B. Walker, C. Kim and T. Q. Nguyen, *Chem. Mater.*, 2011, **23**, 470; (*d*) S. Loser, C. J. Bruns, H. Miyauchi, R. P. Ortiz, A. Facchetti, S. I. Stupp and T. J. Marks, *J. Am. Chem. Soc.*, 2011, **133**, 8142; (*e*) Y. Li, Q. Guo, Z. Li, J. Pei and W. Tian, *Energy Environ. Sci.*, 2010, **3**, 1427; (*f*) A. Tamayo, T. Kent, M. Tantitiwat, M. A. Dante, J. Rogers and T.-Q. Nguyen, *Energy Environ. Sci.*, 2009, **2**, 1180; (*g*) J.-H. Huang, M. Velusamy, K.-C. Ho, J.-T. Lin and C.-W. Chu, *J. Mater. Chem.*, 2010, **20**, 2820.

4 (*a*) L. L. Xue, J. T. He, X. Gu, Z. F. Yang, B. Xu and W. J. Tian, *J. Phys. Chem. C*, 2009, **113**, 12911; (*b*) Y. Yang, J. Zhang, Y. Zhou, G. J. Zhao, C. He, Y. F. Li, M. Andersson, O. Inganas and F. L. Zhang, *J. Phys. Chem. C*, 2010, **114**, 3701; (*c*) Z. Li, Q. Dong, Y. Li, B. Xu, M. Deng, J. Pei, J. Zhang, F. Chen, S. Wen, Y. Gao and W. Tian, *J. Mater. Chem.*, 2011, **21**, 2159; (*d*) Z. Li, Q. Dong, B. Xu, H. Li, S. Wen, J. Pei, S. Yao, H. Lu, P. Li and W. Tian, *Sol. Energy Mater. Sol. Cells*, 2011, **95**, 2272.

5 (*a*) G. D. Wei, S. Y. Wang, K. Sun, M. E. Thompson and S. R. Forrest, *Adv. Energy Mater.*, 2011, **1**, 184; (*b*) R. Fitzner, E. Reinold, A. Mishra, E. Mena-Osteritz, H. Ziehlke, C. Körner,

K. Leo, M. Riede, M. Weil, O. Tsaryova, A. Weiß, C. Uhrich, M. Pfeiffer and P. Bäuerle, *Adv. Funct. Mater.*, 2011, **21**, 897; (*c*) Y. Matsuo, Y. Sato, T. Niinomi, I. Soga, H. Tanaka and E. Nakamura, *J. Am. Chem. Soc.*, 2009, **131**, 16048; (*d*) L.-Y. Lin, Y.-H. Chen, Z.-Y. Huang, H.-W. Lin, S.-H. Chou, F. Lin, C.-W. Chen, Y.-H. Liu and K.-T. Wong, *J. Am. Chem. Soc.*, 2011, **133**, 15822; (*e*) Y. Liu, X. Wan, F. Wang, J. Zhou, G. Long, J. Tian, J. You, Y. Yang and Y. Chen, *Adv. Energy Mater.*, 2011, **1**, 771; (*f*) V. Steinmann, N. M. Kronenberg, M. R. Lenze, S. M. Graf, D. Hertel, K. Meerholz, H. Bürckstümmer, E. V. Tulyakova and F. Würthner, *Adv. Energy Mater.*, 2011, **1**, 888.

6 C. He, Q. He, Y. Yi, G. Wu, F. Bai, Z. Shuai and Y. Li, *J. Mater. Chem.*, 2008, **18**, 4085.

7 H. Shang, H. Fan, Y. Liu, W. Hu, Y. Li and X. Zhan, *Adv. Mater.*, 2011, **23**, 1554.

8 Z. Lin, J. Bjorgaard, A. G. Yavuz and M. E. Kose, *J. Phys. Chem. C*, 2011, **115**, 15097.

9 Y.-F. Liu, X.-F. Ren, L.-Y. Zou, A.-M. Ren, J.-K. Feng and C.-C. Sun, *Theor. Chem. Acc.*, 2011, **129**, 833.

10 (*a*) J. A. Mikroyannidis, A. N. Kabanakis, S. S. Sharma and G. D. Sharma, *Org. Electron.*, 2011, **12**, 774; (*b*) E. Ripaud, T. Rousseau, P. Leriche and J. Roncali, *Adv. Energy Mater.*, 2011, **1**, 540.

11 (*a*) C.-L. Chang, C.-W. Liang, J.-J. Yu, L. Wang and M.-K. Leung, *Sol. Energy Mater. Sol. Cells*, 2011, **95**, 2371; (*b*) D. Sahu, H. Padhy, D. Patra, J.-H. Huang, C.-W. Chu and H.-C. Lin, *J. Polym. Sci., Part A: Polym. Chem.*, 2010, **48**, 5812.

12 (*a*) D. Deng, Y. Yang, J. Zhang, C. He, M. Zhang, Z.-G. Zhang, Z. Zhang and Y. Li, *Org. Electron.*, 2011, **12**, 614; (*b*) J. Zhang, Y. Yang, C. He, Y. He, G. Zhao and Y. Li, *Macromolecules*, 2009, **42**, 7619.

13 G. L. Wu, G. Zhao, C. He, J. Zhang, Q. He, X. Chen and Y. Li, *Sol. Energy Mater. Sol. Cells*, 2009, **93**, 108.

14 J. Zhang, D. Deng, C. He, Y. He, M. Zhang, Z.-G. Zhang, Z. Zhang and Y. Li, *Chem. Mater.*, 2011, **23**, 817.

15 J. C. Bijleveld, A. P. Zoombelt, S. G. J. Mathijssen, M. M. Wienk, M. Turbiez, D. M. de Leeuw and R. A. J. Janssen, *J. Am. Chem. Soc.*, 2009, **131**, 16616.

16 A. P. Zoombelt, S. G. J. Mathijssen, M. G. R. Turbiez, M. M. Wienk and R. A. J. Janssen, *J. Mater. Chem.*, 2010, **20**, 2240.

17 E. Z. Shimpei, Y. K. Tajima, C. Yang and K. Hashimoto, *Chem. Mater.*, 2009, **21**, 4055.

18 A. B. Tamayo, M. Tantiwiwat, B. Walker and T.-Q. Nguyen, *J. Phys. Chem. C*, 2008, **112**, 15543.

19 (*a*) E. Ripaud, Y. Olivier, P. Leriche, J. Cornil and J. Roncali, *J. Phys. Chem. B*, 2011, **115**, 9379; (*b*) S. K. Lee, J. M. Cho, Y. Goo, W. S. Shin, J.-C. Lee, W.-H. Lee, I.-N. Kang, H.-K. Shim and S.-J. Moon, *Chem. Commun.*, 2011, **47**, 1791; (*c*) I. H. Jung, J. Yu, E. Jeong, J. Kim, S. Kwon, H. Kong, K. Lee, H. Y. Woo and H.-K. Shim, *Chem.–Eur. J.*, 2010, **16**, 3743; (*d*) H. Cha, H. Kong, D. S. Chung, W. M. Yun, T. K. An, J. Hwang, Y.-H. Kim, H.-K. Shim and C. E. Park, *Org. Electron.*, 2010, **11**, 1534.

20 (*a*) A. B. Tamayo, B. Walker and T.-Q. Nguyen, *J. Phys. Chem. C*, 2008, **112**, 11545; (*b*) S. Ko, R. Mondal, C. Risko, J. K. Lee, S. Hong, M. D. McGehee, J.-L. Brédas and Z. Bao, *Macromolecules*, 2010, **43**, 6685.

21 D. Sahu, H. Padhy, D. Patra, D. Kekuda, C.-W. Chu, I.-H. Chiang and H.-C. Lin, *Polymer*, 2010, **51**, 6182.

22 B. C. Thompson and J. M. J. Frechet, *Angew. Chem., Int. Ed.*, 2008, **47**, 58.

23 B. Walker, A. B. Tamayo, X.-D. Dang, P. Zalar, J.-H. Seo, A. Garcia, M. Tantiwiwat and T.-Q. Nguyen, *Adv. Funct. Mater.*, 2009, **19**, 3063.

24 (*a*) Y. Li, H. Li, B. Xu, Z. Li, F. Chen, D. Feng, J. Zhang and W. Tian, *Polymer*, 2010, **5**, 1786; (*b*) Y. Li, L. Xue, H. Li, Z. Li, B. Xu, S. Wen and W. Tian, *Macromolecules*, 2009, **42**, 4491; (*c*) Q. Peng, K. Park, T. Lin, M. Durstock and L. Dai, *J. Phys. Chem. B*, 2008, **112**, 2801.

25 (*a*) K. R. Choudhury, J. Subbiah, S. Chen, P. M. Beaujuge, C. M. Amb, J. R. Reynolds and F. So, *Sol. Energy Mater. Sol. Cells*, 2011, **95**, 2502; (*b*) V. D. Mihailetchi, J. Wildeman and P. W. M. Blom, *Phys. Rev. Lett.*, 2005, **94**, 126602.

26 J. A. Mikroyannidis, D. V. Tsagkournos, S. S. Sharma, Y. K. Vijay and G. D. Sharma, *Org. Electron.*, 2010, **11**, 2045.

27 J. Hou, T. L. Chen, S. Zhang, H.-Y. Chen and Y. Yang, *J. Phys. Chem. C*, 2009, **113**, 1601.

28 (*a*) H. Fan, H. Shang, Y. Li and X. Zhan, *Appl. Phys. Lett.*, 2010, **97**, 133302; (*b*) J. Kettle, M. Horie, L. A. Majewski, B. R. Saunders, S. Tuladhar, J. Nelson and M. L. Turner, *Sol. Energy Mater. Sol. Cells*, 2011, **95**, 2186.

29 F.-C. Chen, H.-C. Tseng and C.-J. Ko, *Appl. Phys. Lett.*, 2008, **92**, 103316-1.

30 L. Li, H. Tang, H. Wu, G. Lu and X. Yang, *Org. Electron.*, 2009, **10**, 1334.